New Large-Area Mapping Techniques with Mopra

Peter Barnes (University of Florida) and Tom Dame (Center for Astrophysics)

14th October 2009

This memo reports new large-area mapping techniques we have developed at Mopra, primarily for our project M395 on mapping the Far 3-kpc Arm (F3A), but also mindful of the community interest in applying any such new techniques to some of the MALT-related projects discussed in various meetings in 2008 & 2009. The two new techniques we describe are choosing the "Nyquist frequency" to be well below the observing frequency, in order to direct the OTF system to make larger maps than usual, and to further adjust the Nyquist frequency by smaller amounts to make OTF maps all with the same sensitivity by allowing for variations in observing conditions, especially due to elevation.

1 Overview of the Problem

In its on-the-fly (OTF) mapping mode, the maximum scanning speed at which the Mopra telescope can Nyquist-sample a given area of sky depends primarily on two parameters: the observing frequency ν_o (typically the central frequency of the MOPS correlator, but optionally any frequency within the range being correlated by MOPS) and the sample time t_s (i.e., the interval between data dumps from the correlator). This translates to a typical scanning speed along each OTF row of about $6''\mathrm{sec}^{-1}$ at 90 GHz, and the time required to build (for example) a $6'\times6'$ OTF map is, from experience, approximately

$$ t_m \;\; = \;\; 80\,\mathrm{min}\left(\frac{\nu_o}{90\,\mathrm{GHz}}\right)^2\left(\frac{t_s}{2\,\mathrm{s}}\right)\;. \tag{1} $$

The time required for maps of different size would scale in rough proportion to the map's area. As it turns out, this mapping speed is quite adequate to produce reduced data cubes of reasonably small rms noise σ with only 1 or 2 overlaid OTF maps, at all frequencies from 18 to 116 GHz, under reasonable observing conditions. For example at 90 GHz in zoom mode, the data cube represented by eq. 1 would have roughly

$$ \sigma(90\,\mathrm{GHz}) \;\; = \;\; 0.3\,\mathrm{K}\left(\frac{T_{sys}}{200\,\mathrm{K}}\right)\left(\frac{0'.6}{\theta_G}\right)\;\;\text{per channel, per pixel} \tag{2} $$

as measured on the usual T_A^* scale, and after processing through Livedata & Gridzilla with typical gridding parameters (this is explained in more detail in Tony Wong's OTF memo from 2005, where multiple t_s samples contribute to each gridded pixel under various gridding schemes). Here we have also used a gridding kernel of size θ_G as shown, appropriate for 90 GHz. The gridding kernel matters because for the same input data, as θ_G gets larger more samples are included in the gridded pixel's final value. Thus the map noise decreases as the inverse-square-root of the kernel's area, or as one over the gridding kernel size. At other frequencies, the noise scales by the atmospheric opacity as well as the receiver performance. However, this is already incorporated into the T_{sys} factor.

Until recently the t_s factor in eq. 1 was ignored since it was assumed to be immutable. However recent discussions among the astronomical community and ATNF engineeering staff have opened the possibility of substantially decreasing this factor, potentially greatly speeding up Nyquist-sampled

mapping at Mopra. The penalty one pays is in the noise figure: σ in each t_s-long sample will obviously increase as $(t_s)^{-0.5}$, and the noise in the final map will rise by the same factor. (Equivalently, reducing the sample time t_s will decrease the total map time t_m by roughly the same factor, although the overheads will not necessarily scale in the same way.) Therefore we can rewrite eq. 2 as

$$\sigma(90\,\text{GHz}) = 0.3\,\text{K}\left(\frac{T_{sys}}{200\,\text{K}}\right)\left(\frac{0'.6}{\theta_G}\right)\left(\frac{80\,\text{m}}{t_m}\right)^{0.5} \text{ per channel, per pixel} \tag{3}$$

$$= 0.3\,\text{K}\left(\frac{T_{sys}}{200\,\text{K}}\right)\left(\frac{0'.6}{\theta_G}\right)\left(\frac{90\,\text{GHz}}{\nu_o}\right)\left(\frac{2\,\text{s}}{t_s}\right)^{0.5} \text{ per channel, per pixel}, \tag{4}$$

where normally $\theta_G \approx \theta_o$, the telescope beam FWHM at the observing frequency ν_o.

2 Pseudo-Fast-Mapping

For M395 we wanted to map a $3°\times0°.5$ area of the F3A but only had time to map $0°.5\times0°.5$ at the limited speed of normal OTF mapping. However the OTF perl script accepts a parameter, the "Nyquist frequency" (ν_N), which can be employed to get around this limitation, in the case where one is mapping extended emission and true Nyquist sampling is not essential to one's goals. Normally one uses a ν_N which is near ν_o in order to guarantee properly-sampled maps. But since we were primarily interested in mapping the bright ^{12}CO line, which is usually quite widely-distributed, its fine-scale structure could be averaged over in order to find the overall extent of the emission. Therefore we could use a much **lower** ν_N to sample the CO emission more sparsely than Nyquist. As it turned out, our sampling was only slightly larger than the Mopra beam at 115 GHz, which gave an effective resolution $\sim1.5'$, still substantially better than the well-known CfA or Nanten large-area surveys. (**Note:** the argument has also been made that Nyquist-sampling is necessary for more typical line strengths of $\sim$1–3 K in order to maintain a reasonable S/N. But as we show below this is not the case. Our techniques are thus useful for any line strength, as long as one can do without Nyquist sampling.)

Since we were still limited to $t_s = 2\,\text{s}$, for our observations we substituted a much smaller $\nu = \nu_N$ for ν_o in eq. 4, typically $\sim$40 GHz instead of 115 GHz. As can be seen from eqs. 1 & 4, lowering the ν_N to an nth of ν_o raises σ by the same factor, but saves a factor n^2 in observing time. We therefore see that we pay a relatively small noise penalty to gain a large increase in mapping speed. (However as we shall see below, we can use a larger θ_G to eliminate even this penalty.) We call this mode (which is independent of the true FM capability that we presume will soon be available at Mopra) **"pseudo-Fast-Mapping"**, or **psFM**, and as we show here it is available now.

In psFM, as the telescope scans along each OTF row, the receiver is integrating the signal continuously in the scanning direction. Therefore although the dump rate to mass storage is too slow to keep up with the Nyquist criterion at the "fast" scanning speed corresponding to a "low" ν_N, the data dumped per sample are nevertheless a true average of the sky emission along the scan row. This means that each row will effectively be convolved to a resolution corresponding to the Mopra beam at the ν_N, rather than to the beam at ν_o.

However the low ν_N also means that adjacent rows are spaced appropriately for the same lower frequency; thus the map will undersample the true sky brightness distribution orthogonally to the scan rows, compared to the telescope beam at ν_o. In Gridzilla therefore, one should scale θ_G to ν_N rather than to ν_o; in this way one averages into each gridded pixel several samples, both along **and** across rows. The resulting map will approximate a convolved version of a normal slow OTF map made with

$\nu_N = \nu_o$, although it won't be a true convolution of the sky due to the undersampling feature of psFM. More importantly, this improves our psFM performance even further than described above. Eq. 4 then looks like

$$\sigma(90\,\text{GHz}) \;=\; 0.3\,\text{K}\left(\frac{T_{sys}}{200\,\text{K}}\right)\left(\frac{0'.6}{\theta_G}\right)\left(\frac{90\,\text{GHz}}{\nu_N}\right)\left(\frac{2\,\text{s}}{t_s}\right)^{0.5} \text{ per channel, per pixel}. \qquad (5)$$

Now we substitute $\theta_G = \theta_o\nu_o/\nu_N$, where θ_o is the telescope's beamwidth at ν_o, to get

$$\sigma(90\,\text{GHz}) \;=\; 0.3\,\text{K}\left(\frac{T_{sys}}{200\,\text{K}}\right)\left(\frac{0'.6}{\theta_o\nu_o}\right)\nu_N\left(\frac{90\,\text{GHz}}{\nu_N}\right)\left(\frac{2\,\text{s}}{t_s}\right)^{0.5} \text{ per channel, per pixel} \qquad (6)$$

$$\;=\; 0.3\,\text{K}\left(\frac{T_{sys}}{200\,\text{K}}\right)\left(\frac{0'.6}{\theta_o}\right)\left(\frac{90\,\text{GHz}}{\nu_o}\right)\left(\frac{2\,\text{s}}{t_s}\right)^{0.5} \text{ per channel, per pixel}, \qquad (7)$$

which is the same as eq. 4: the resulting map σ should then be the same as in the slow OTF mapping case. This makes sense since we are spending the same amount of clock time with the same equipment, but using it to map a larger area of sky, so the noise level per effective resolution element should be the same.
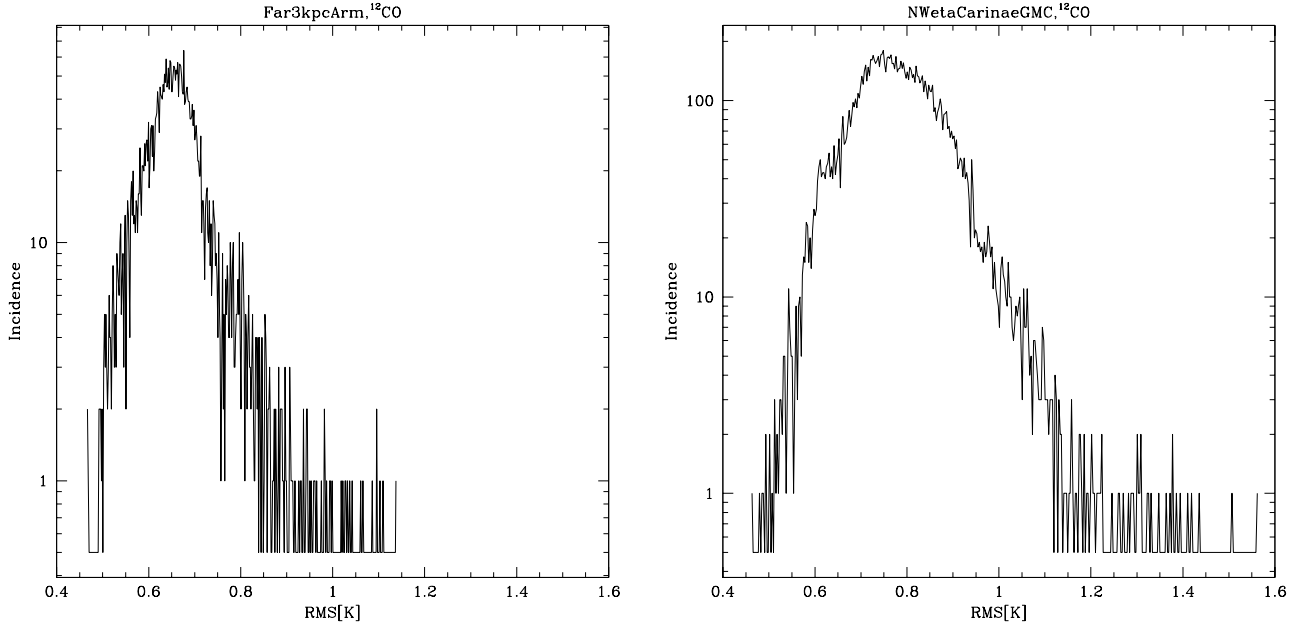

Figure 1: RMS noise histograms (log scale) for psFM (above left) and normal OTF (above right) maps.

3   Results

To illustrate how well this works, we compare a psFM map with a normal OTF map, made under similarly good observing conditions, when $T_{sys} \sim 450\,\text{K}$ at 115 GHz. For the F3A we mapped $12'\times 12'$ areas with $\nu_N \sim 40\,\text{GHz}$ during 2009 July in about the same time that a normal "slow-mapped" OTF map of size $4'\times 4'$ would take at $\nu_N = 115\,\text{GHz}$, i.e. about 90 min. For this F3A map we used a gridding kernel of $150''$ instead of the more usual $30''$ for 115 GHz, which gave good sampling in the resulting data cube. (This large gridding kernel was for convenience only; kernels below $90''$ for the

same F3A data also worked well.) Therefore the noise figure for this map is expected to be $\sim 0.6\times$ that suggested by eq. 5, since the gridding kernel was 5/3 as large as the ν_N would have dictated. To compare we have a map from CHaMP at 115 GHz taken in 2009 April, but where 2 OTF maps were typically combined for each field; therefore its noise figure is expected to be $\sim 0.71\times$ the eq. 5 level. We show in Figure 1 noise histograms from each of these maps in the ^{12}CO line, although these are now both on the T_R^* scale, which $= T_A^*/0.55$ for extended sources. Here it can be seen that the modal rms value is indeed slightly less in the psFM map than in the regular slow map, 0.65 K vs. 0.75 K, very close to what was expected!
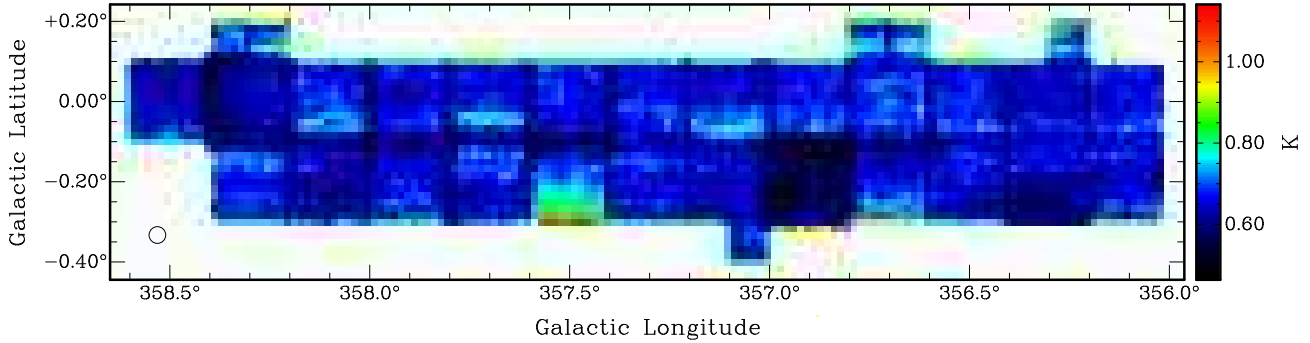

Figure 2: RMS noise maps for psFM (above) and normal OTF mapping (right), each over a large number of OTF fields (26 & 16 resp.). For the psFM map, there is only one modal peak in the rms at 0.65 K. For the normal OTF map, the modal rms is 0.75 K, but there is a much larger variation in rms than in the psFM map due to the rms' strong elevation dependence. There are also (blended) secondary peaks in the histogram at 0.85 K due to poor weather for one OTF field, and at 0.65 K due to excess coverage for another field (see also Fig. 1).
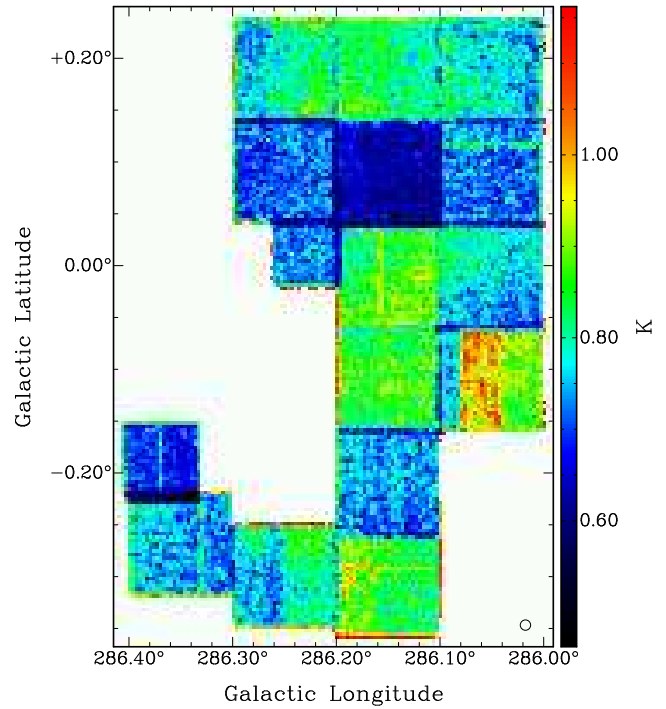
4 Fine-Tuning the RMS

Figure 1 shows another feature of large-scale maps that many users have struggled with, which is the variation of σ within a map. This is apparent in the substantially larger dispersion in the rms for the normal OTF data on the right, compared to the much narrower rms-dispersion on the psFM plot to the left. With normal OTF one sees broader shoulders in the histogram both at lower and higher rms than the peak, due to atmospheric opacity variations with elevation, but also due to variable weather or coverage. Usually the science that can be obtained from mm-wave maps is limited by the worst noise level in the map. Ideally therefore, one wants the integration time adjusted so that the noise

level is as even as possible across the map. Any portion of one's map with better noise is not so useful in comparison to other portions, and so is almost time wasted. Portions with worse noise detract from the impact of conclusions that might otherwise be formed from the less noisy parts. Thus an observing strategy that smoothes out noise variations as far as possible is the most efficient in converting valuable telescope time into science.

Eq. 5 gives us a method to easily achieve this goal as well. Because the noise scales inversely with the ν_N, users have the option of **adjusting, for each OTF map, the ν_N in proportion to the current T_{sys}**, while keeping the map size fixed. It can be seen that the ν_N and T_{sys} factors exactly cancel in eq. 5, trivially giving us the desired result of a constant σ for every OTF map. Effectively, we are adjusting the total integration time for the fixed-sized OTF map by adjusting the grid spacing. The T_{sys} at the end of the previous OTF map can be used for the adjustment, and one can do even slightly better by using the projected average T_{sys} during the OTF map; this can be estimated by assuming the usual constant-plus-cosecant dependence (in good conditions) of T_{sys} on elevation. In poor weather this will be more difficult of course. In Figure 2 we give examples of these two approaches. Note the variation in σ is far less in the ν_N-T_{sys}-tuned psFM than in the normal $\nu_N = \nu_o$ slow map. This can also be seen in Figure 1, where the psFM histogram has essentially only one normal distribution, whereas the slow, untuned map has multiple, blended distributions apart from the dominant one, due to the variable sky coverage without reference to the extant T_{sys}.

To emphasise this, we can extract these factors from eq. 5 and write

$$\nu_N = \nu_N(\text{avg}) \left(\frac{T_{sys}}{T_{sys}(\text{avg})} \right). \tag{8}$$

The $T_{sys}(\text{avg})$ (perhaps 450 K for CO in good conditions) is just the average T_{sys} expected for a particular project. It will depend on the observing frequency and the elevation track of the map region. The $\nu_N(\text{avg})$ (we used 43 GHz for our F3A project) is the all-important factor, and determines the sensitivity per unit area and the grid spacing. In principle one can start with the total area one wants to map and the total amount of observing time available and calculate the $\nu_N(\text{avg})$. Of course the resulting grid spacing needs to remain well below the angular resolution that one requires (given by the smoothing kernel).

5 Summary of psFM

Our new techniques provide two important advantages over normal OTF: one can map a much larger area in the same amount of time if one does not require Nyquist-sampled maps, and one can do so with nearly uniform sensitivity per unit area. The first technique makes possible a whole array of science projects not considered feasible beforehand. Without the second technique, normal OTF provides no way of compensating for changes in Tsys other than the very clumsy and inefficient method of repeating whole maps. For uniform large-scale mapping psFM is far more efficient than normal OTF, making near-optimum use of telescope time. As an additional bonus, every region is only mapped once, cutting down on telescope slew time, additional test scans, data processing, and bookeeping.

We can recast eq. 5 into a form which can be normalised as users find convenient, for whatever observing frequency and gridding preference, and which allows psFM to be performed in a way that takes account of conditions, maximising Mopra's large-scale mapping efficiency. Although this is similar to the Radiometer Equation, because of the peculiarities of the Mopra OTF system (especially

the use of θ_G in Gridzilla) it is worth defining as a separate formula. For this reason we suggest naming it the **Mopra Mapping Equation:**

$$\sigma \;=\; K\,\frac{T_{sys}}{\theta_G\,\nu_N\,\sqrt{t_s}} \text{ per channel, per pixel,} \tag{9}$$

where K = 0.115 K arcmin s$^{-1.5}$ when the input quantities are measured in K, arcmin, GHz, and seconds. This value of K is optimised for 3mm work; further study at (e.g.) longer wavelengths may reveal that it needs to be recalibrated in those cases.

6 True Fast-Mapping

The Mapping Equation is easily extended once true FM becomes available at Mopra, i.e. when t_s can be chosen much smaller than the traditional 2 s. Suppose t_s = 0.2 s is available, then clearly the σ per sample time will be $\sim$3$\times$ worse. With the same large gridding kernel as with psFM, we would of course recover the same noise figure as before, but simply from 10$\times$ as much data, and with the resolution of the map still effectively that for the lower ν_N. But by returning the ν_N to ν_o, we recover the full resolution of the Mopra telescope, although now σ in the final map (with a smaller gridding kernel) is $\sim$3$\times$ higher than with psFM. However this is what was desired since typically FM will be used on bright lines such as ^{12}CO or ^{13}CO, where a somewhat higher noise figure can be tolerated. In this instance the $\nu_N \sim \nu_o$ can still be adjusted if desired as the T_{sys} varies, in order to smooth out the noise variations in the true fast map. Therefore the Mopra Mapping Equation as described here is equally capable of guiding observers with normal OTF, psFM, or true FM.